Passive seismic imaging in the presence of white noise sources: numerical simulations

Deyan Draganov, Kees Wapenaar, and Jan Thorbecke, Delft University of Technology, Department of Applied Earth Sciences*

Summary

Passive seismic imaging is based on the relation between the reflection and the transmission responses of the subsurface. By cross-correlating the transmission responses of a 3-D inhomogeneous medium in the presence of white noise sources, measured at points A and B, one can simulate the reflection response of the same medium as if measured at point A in the presence of an impulsive source at point B. In this paper we show by numerical simulations that the received reflection response strongly depends on the whiteness of the sources. Reflectors present beneath the noise sources cause some ghost events to appear. Random distribution of the noise sources weakens these ghost reflections.

Introduction

One of the applications of the general relations between the reflection and the transmission response of a medium is in passive seismic imaging. Claerbout (1968) derived the relation for a horizontally layered medium. In Wapenaar et al. (2002) a relation was derived between the reflection and transmission response for a 3-D inhomogeneous medium in the presence of uncorrelated white noise sources in the subsurface. In the derivation it was assumed that there are no reflectors beneath the sources. In this paper, we show some numerical modeling results with reflectors beneath the sources.

Simulating reflection from transmission

Let us have 3-D inhomogeneous domain $\mathcal{D}$, which is lossless and source free (see Figure 1), embedded between plan parallel boundaries $\partial\mathcal{D}_0$ and $\partial\mathcal{D}_m$. Just above $\partial\mathcal{D}_0$ we have a free surface and below $\partial\mathcal{D}_m$ the half space is homogeneous. For this configuration, the reflection response can be calculated from the transmission response in the time domain using the relation (Wapenaar et al., 2002)

$$R(\boldsymbol{x}_A,\boldsymbol{x}_B,t)+R(\boldsymbol{x}_A,\boldsymbol{x}_B,-t)=\delta(\boldsymbol{x}_{H,B}-\boldsymbol{x}_{H,A})\,\delta(t)-\int_{\partial\mathcal{D}_m} T(\boldsymbol{x}_A,\boldsymbol{x},-t)*T(\boldsymbol{x}_B,\boldsymbol{x},t)\,d\boldsymbol{x}. \quad (1)$$

In this equation, $R(\boldsymbol{x}_A,\boldsymbol{x}_B,t)$ denotes the reflection response including all free-surface and internal multiples of the domain $\mathcal{D}$ in the presence of a source at $\boldsymbol{x}_A$ and a receiver at $\boldsymbol{x}_B$ (Figure 1). $T(\boldsymbol{x}_A,\boldsymbol{x},t)$ denotes the transmission response including all free-surface and internal multiples of the domain $\mathcal{D}$ in the presence of a source at $\boldsymbol{x}$ and a receiver at $\boldsymbol{x}_A$ (see Figure 2); $*$ symbolizes convolution; $\boldsymbol{x}_{H,A}$ symbolizes the horizontal coordinates x_1 and x_2 of point A. The points with position vector $\boldsymbol{x}_A$ and $\boldsymbol{x}_B$ are situated just above the surface $\partial\mathcal{D}_0$. In the derivation of this relation, the evanescent wave modes have been neglected. If the integral over the sources is discretized and the sources are assumed to be white and uncorrelated, equation (1) can be rewritten as

$$R(\boldsymbol{x}_A,\boldsymbol{x}_B,t)+R(\boldsymbol{x}_A,\boldsymbol{x}_B,-t)=\delta(\boldsymbol{x}_{H,B}-\boldsymbol{x}_{H,A})\,\delta(t)-T_{obs}(\boldsymbol{x}_A,-t)*T_{obs}(\boldsymbol{x}_B,t). \quad (2)$$

Here,

$$T_{obs}(\boldsymbol{x}_A,-t)=\sum_{\boldsymbol{x}_i\in\partial\mathcal{D}_m} T(\boldsymbol{x}_A,\boldsymbol{x}_i,-t)*N_i(-t) \quad (3)$$

$$T_{obs}(\boldsymbol{x}_B,t)=\sum_{\boldsymbol{x}_j\in\partial\mathcal{D}_m} T(\boldsymbol{x}_B,\boldsymbol{x}_j,t)*N_j(t) \quad (4)$$

represent the transmission response of domain $\mathcal{D}$ recorded at $\partial\mathcal{D}_0$ in the presence of a number of discretely distributed uncorrelated white noise sources. In equation (2) the sources are along the boundary $\partial\mathcal{D}_m$, but because the correlation process eliminates the extra travel times, the sources can be randomly distributed. (see Figure 3).

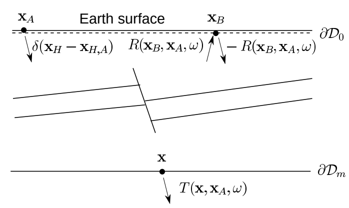

Fig. 1: *Domain $\mathcal{D}$ with its reflection response observed at the surface and with its transmission response observed in the subsurface.*

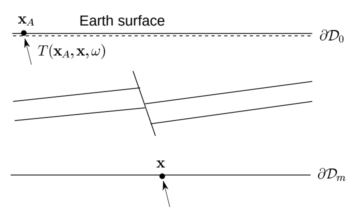

Fig. 2: *Domain $\mathcal{D}$ with its transmission response observed at the surface.*

In the derivation of equation (2) it was assumed that the medium beneath the lower boundary $\partial\mathcal{D}_m$ of domain $\mathcal{D}$ is homogeneous, i.e. that there are no reflectors. What will happen if reflectors are present beneath the sources?

In the following, we show some 2-D modelling results. As a model are taken three layers with the first two layers separated with an anticline-shaped boundary. The acoustic velocity and the density for the layers are: top layer - 1500 $\frac{m}{s}$ and 1000 $\frac{kg}{m^3}$; middle layer - 2000 $\frac{m}{s}$ and 3000 $\frac{kg}{m^3}$; bottom layer- 2800 $\frac{m}{s}$ and 4000 $\frac{kg}{m^3}$. The receivers are regularly spaced at the surface at every 20 m starting at position 1200 m.

Figure 4 shows the described model with three clusters of white noise sources at depth level 750 m. This model can be seen as an anticline reservoir with noise sources resulting from hydraulic fracturing. The first cluster is situated between horizontal distances 2500 and 3000 m, the second - between 3750 and 4250 m, the third - between 5000 and 5500 m. There are 101 sources within each cluster with distance between sources of 5 m. Using relation (2) we can calculated the reflection response R of the subsurface from the transmission response T_{obs} resulting from all the sources (see Figure 5). In the following examples 66 minutes long transmission records were used. After cross-correlating the transmission records and muting the non-causal part we obtain the simulated reflection response as shown on Figure 6. This panel simulates a split-spread reflection survey with a source at 4000 m. The presence of the extra reflector at 900 m causes additional reflection events to appear in the simulated reflection response. Comparing the simulated reflection with the directly modelled reflection response (Figure 7) one can see that some of the events represent correctly real reflections, while others are ghost events. Ghosts are present on the simulated reflection response before the first reflection event. The ghost event with apex at 0.15 s is a consequence from the source field being reflected at the layer beneath the sources. The event at 0.45 s is an internal multiple between the first and the third layers. The ghost reflection at 0.6 s comes from the reflection from the bottom of the model. One can further see multiples from these ghosts present in the picture. There is an extra ghost event with an apex at 0.37 s.

Figure 9 shows the simulated reflection response for the same model, but now the depth coordinates of the sources in each cluster are randomly distributed between levels 700 m and 800 m (see Figure 8). Comparing this simulation with Figure 6, we see that the mentioned ghost events are nearly absent, except for the events with apexes at 0.45 and 0.37 s. Note, that the reflections that were correctly represented in Figure 6 are still correctly represented in the simulated reflection response in Figure 9.

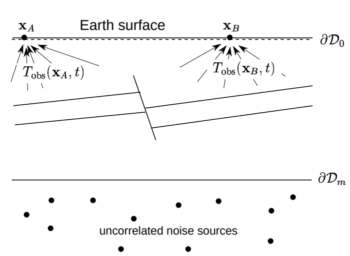

Fig. 3: *Transmission response recorded at positions $\boldsymbol{x}_A$ and $\boldsymbol{x}_B$ in the presence of white noise sources in the subsurface.*

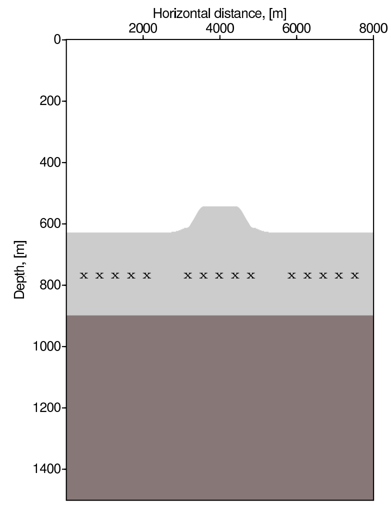

Fig. 4: *Anticline model with white noise sources in three clusters. In the clusters the sources are regularly distributed.*

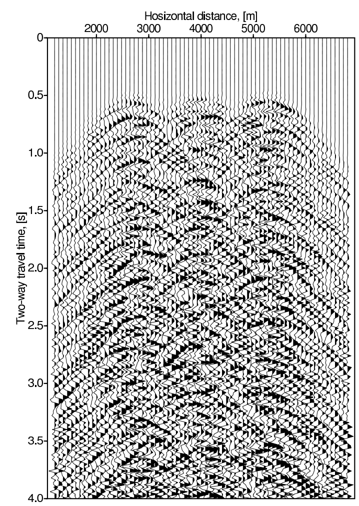

Fig. 5: *First 4 s from the 66 minutes long transmission panel (T_{obs}) from white noise sources in the subsurface*

Figure 10 shows the anticline model with sources distributed each 25 m between horizontal positions 1200 m and 6800 m. The depth coordinates of the sources are randomly distributed between levels 700 m and 800 m. In Figure 11 we can see that the ghost event with apex at 0.37 s is eliminated, i.e. this event was a result from the big gaps between the clusters. The ghost event with apex at 0.36 s and its multiple are still present. It results from the internal reflection of the source field between the first and the third layer before it is registered at the surface. The ghost events that were eliminated resulted from source fields reflected from the boundaries beneath the sources and have not experienced internal multiple reflection on their way to the surface.

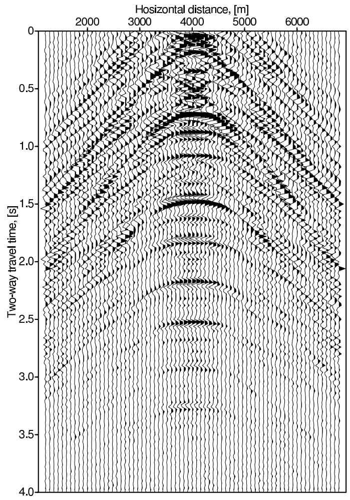

Fig. 6: *Simulated reflection response for the model on figure 4.*

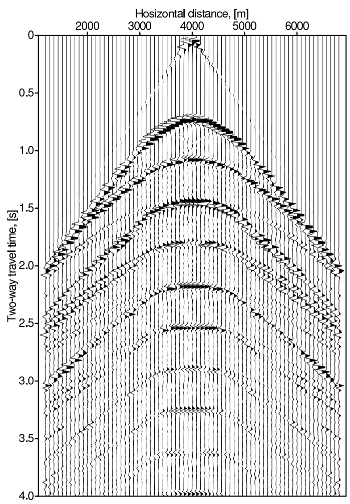

Fig. 7: *Directly modelled reflection response for the three layers model with source at the surface at position 4000 m.*

The quality of the synthesized reflection response depends also on the concentration of the sources in groups (see model on Figure 8). Figure 12 shows the simulated reflection response of the model when only white noise sources from the left and the middle clusters are active. On the other hand, when we record transmission responses from the left and the right clusters we can construct a reflection response as shown on Figure 13. The hyperbolic events are party visible depending on the angle of "exposure" of the anticline to the sources.

Conclusions

The numerical modelling results in this paper confirm relation (2) between the reflection and the transmission responses of a 3-D inhomogeneous lossless medium in

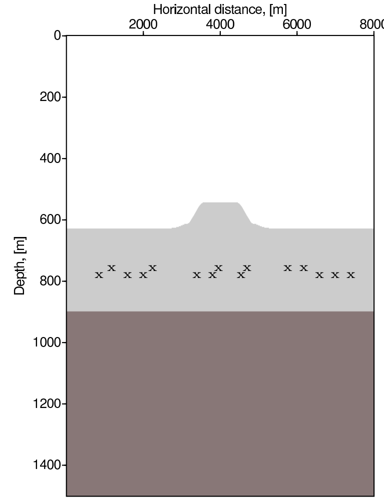

Fig. 8: *Anticline model with white noise sources in three clusters. In the clusters the sources are randomly distributed in the vertical direction and regularly distributed in the horizontal direction (for each cluster only 5 out of 101 sources are shown).*

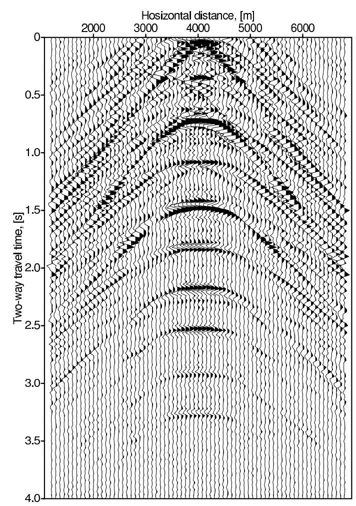

Fig. 9: *Simulated reflection response for the model on figure 8.*

the presence of white noise sources. When reflectors are present beneath the sources, additional reflections, some of which are ghosts, appear in the simulated reflection response. The ghost events are strongly weakened, however, when the white noise sources have randomly distributed depths, while the real reflections are still correctly represented. Big gaps in the horizontal distribution of the white noise sources also cause ghost reflections to appear in the simulated reflection survey. It is important to have sources "exposing" the structure of interest from all the angles. The effect of internal

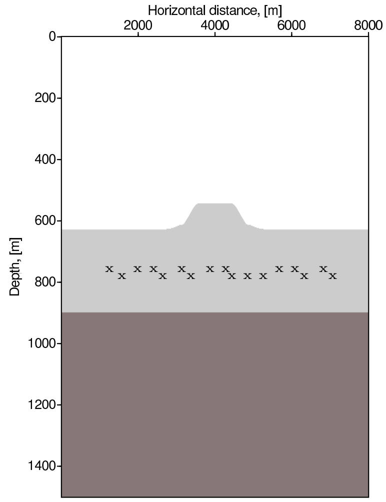

Fig. 10: *Anticline model with white noise sources regularly distributed in the horizontal direction (no gaps between the clusters as in Figure 8). In the vertical direction the sources are with random distributed depths.*

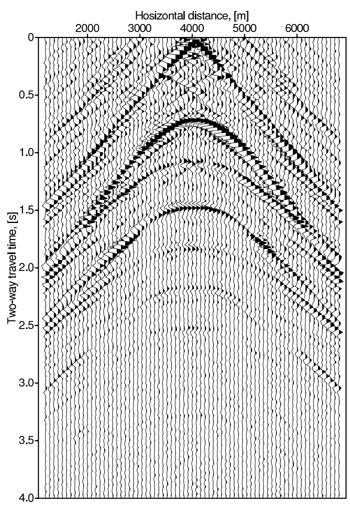

Fig. 11: *Simulated reflection response for the model in figure 10.*

multiples in the transmission data before the first free surface reflection need to be further investigated.

Acknowledgments

This modelling was done as part of a research project financed by the Dutch Science Foundation STW (number DTN4915) and the Netherlands Research Centre for Integrated Solid Earth Sciences - ISES.

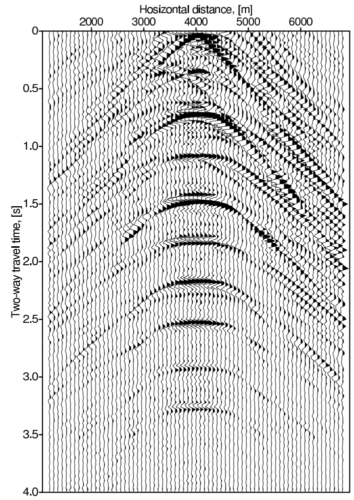

Fig. 12: *Simulated reflection response for the model on Figure 8 when only sources from the left and the middle clusters are present.*

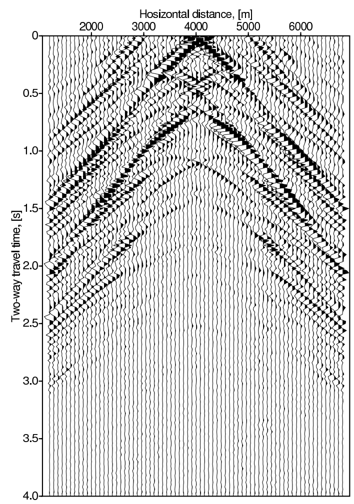

Fig. 13: *Simulated reflection response for the model on Figure 8 when only sources from the left and the right clusters are present.*

References

Claerbout, J. F., 1968, Synthesis of a layered medium from its acoustic transmission response: Geophysics, **33**.

Wapenaar, C. P. A., Thorbecke, J. W., Draganov, D., and Fokkema, J. T., 2002, Theory of acoustic daylight imaging revisited: 72nd Ann. Internat. Mtg., Soc. Expl. Geophys., Expanded abstracts ST 1.5.